

# ATLAS Sensitivity to Leptoquarks, $W_R$ and Heavy Majorana Neutrinos in Final States with High- $p_T$ Dileptons and Jets with Early LHC Data at 14 TeV proton-proton collisions

Vikas Bansal (ATLAS Collaboration)

University of Pittsburgh, 3941 O'Hara St., Pittsburgh, PA 15260, USA

Dilepton-jet final states are used to study physical phenomena not predicted by the standard model. The ATLAS discovery potential for leptoquarks and Majorana Neutrinos is presented using a full simulation of the ATLAS detector at the Large Hadron Collider. The study is motivated by the role of the leptoquark in the Grand Unification of fundamental forces and the see-saw mechanism that could explain the masses of the observed neutrinos. The analysis algorithms are presented, background sources are discussed and estimates of sensitivity and the discovery potential for these processes are reported.

## 1. Introduction

The Large Hadron Collider (LHC) will soon open up a new energy scale that will directly probe for physical phenomena outside the framework of the Standard Model (SM). Many SM extensions inspired by Grand Unification introduce new, very heavy particles such as leptoquarks. Extending the SM to a larger gauge group that includes, *e.g.* Left-Right Symmetry (LRS) [1], could also explain neutrino masses via the see-saw mechanism. The LRS-based Left-Right Symmetric Model (LRSM) [10] used as a guide for presented studies, extends the electroweak gauge group of the SM from  $SU(2)_L \times U(1)_Y$  to  $SU(2)_L \times SU(2)_R \times U(1)_{B-L}$  and thereby introduces  $Z'$  and right-handed  $W$  bosons. If the LRS breaking in nature is such that all neutrinos become Majoranas, the LRSM predicts the see-saw mechanism [2] that elegantly explains the masses of the three light neutrinos.

## 2. Search for scalar leptoquarks

Leptoquarks (LQ) are hypothetical bosons carrying both quark and lepton quantum numbers, as well as fractional electric charge [3, 4]. Leptoquarks could, in principle, decay into any combination of any flavor lepton and any flavor quark. Experimental limits on lepton number violation, flavor-changing neutral currents, and proton decay favor three generations of leptoquarks. In this scenario, each leptoquark couples to a lepton and a quark from the same SM generation[5]. Leptoquarks can either be produced in pairs by the strong interaction or in association with a lepton via the leptoquark-quark-lepton coupling. Figure 1 shows Feynman diagrams for the pair production of leptoquarks at the LHC.

This contribution describes the search strategy for leptoquarks decaying to either an electron and a quark or a muon and a quark leading to final states with two leptons and at least two jets. The branching fraction

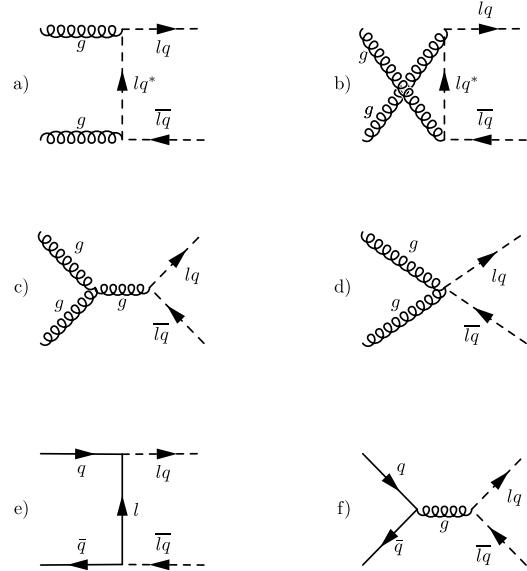


Figure 1: Feynman diagrams for the pair production of scalar leptoquarks via gluon-gluon fusion (a-d) and quark anti-quark annihilation (e-f).

of a leptoquark to a charged lepton and a quark is denoted as  $\beta^1$ .

MC-simulated signal events have been studied[6] using Monte Carlo (MC) samples for first generation (1st gen.) and second generation (2nd gen.) scalar leptoquarks simulated at four masses of 300 GeV, 400 GeV, 600 GeV, and 800 GeV with the MC generator PYTHIA [7] at 14 TeV  $pp$  center-of-mass energy. The next to leading order (NLO) cross section [8] for the above simulated signal decreases with leptoquark mass from a few pb to a few fb with mass point of 400 GeV at  $(2.24 \pm 0.38)$  pb.

<sup>1</sup> $\beta = 1$  would mean that leptoquarks do not decay into quarks and neutrinos.

Table I Partial cross-section (pb) that remains after each selection criterion for the first generation leptoquark channel. Baseline selection corresponds to the first selection of two electron candidates and two jets from the reconstructed objects. The  $Z/DY$  cross section is for the region  $M(ee) \geq 60$  GeV. VB pairs corresponds to the diboson processes of  $WW$ ,  $WZ$ , and,  $ZZ$ .

Physics sample	Before selection	Baseline selection	$S_T \geq 490$ GeV	$M_{ee} \geq 120$ GeV	$M_{lj}^1 - M_{lj}^2$ mass window [ 320-480 ] - [ 320-480 ] [GeV]
LQ (400 GeV)	2.24	1.12	1.07	1.00	0.534
$Z/DY \geq 60$ GeV	1808.	49.77	0.722	0.0664	0.0036
$t\bar{t}$	450.	3.23	0.298	0.215	0.0144
VB pairs	60.94	0.583	0.0154	0.0036	0.00048
Multijet	$10^8$	20.51	0.229	0.184	0.0

Table II Partial cross-section (pb) that remains after each selection criterion for the second generation leptoquark channel. Baseline selection corresponds to the first selection of two muon candidates and two jets from the reconstructed objects. The  $Z/DY$  cross section is for the region  $M(\mu\mu) \geq 60$  GeV. VB pairs corresponds to the diboson processes of  $WW$ ,  $WZ$ , and  $ZZ$ .

Physics sample	Before selection	Baseline selection	$p_T^\mu \geq 60$ GeV $p_T^{jet} \geq 25$ GeV	$S_T \geq 600$ GeV	$M(\mu\mu) \geq 110$ GeV	$M_{lj}$ mass window [ 300 - 500 ] [GeV]
LQ (400 GeV)	2.24	1.70	1.53	1.27	1.23	0.974
$Z/DY \geq 60$ GeV	1808.	79.99	2.975	0.338	0.0611	0.021
$t\bar{t}$	450.	4.17	0.698	0.0791	0.0758	0.0271
VB pairs	60.94	0.824	0.0628	0.00846	0.00308	0.00205
Multijet	$10^8$	0.0	0.0	0.0	0.0	0.0

## 2.1. Reconstruction and objects selection

Signal reconstruction requires selection of two high quality leptons and at least two jets. Each signal jet and lepton candidate is required to have transverse momentum ( $p_T$ )  $> 20$  GeV. This helps to suppress low  $p_T$  background predicted by the SM. Leptons are required to have pseudorapidity  $|\eta|$  below 2.5, which is the inner detector's acceptance, whereas jets are restricted to  $|\eta| < 4.5$  to suppress backgrounds from underlying event and minimum bias events that dominate in the forward region of the detector. In addition, leptons are required to pass identification criteria, which, in case of electrons, are based on electromagnetic-shower shape variables in the calorimeter and, in the case of muons, are based on finding a common track in the muon spectrometer and the inner detector together with a muon isolation<sup>2</sup> requirement in the calorimeter. Electron candidates are also required to have a matching track in the

inner detector. Furthermore, it is required that signal jet candidates are spatially separated from energy clusters in the electromagnetic calorimeter that satisfy electron identification criteria. Finally, a pair of leptoquark candidates are reconstructed from lepton-jet combinations. Given the fact that these four objects can be combined to give two pairs, the pair that has minimum mass difference between the two leptoquark candidates is assumed to be the signal.

## 2.2. Background Studies

The main backgrounds to the signal come from  $t\bar{t}$ , and  $Z/DY$ +jets production processes. Multijet production where two jets are misidentified as electrons, represents another background to the dielectron(1st gen.) channel. In addition, minor contributions arise from diboson production. Other potential background sources, such as single-top production, were also studied and found to be insignificant.

The backgrounds are suppressed and the signal significance is improved by taking advantage of the fact that the final state particles in signal-like events have relatively large  $p_T$ . A scalar sum of transverse momenta of signal jets and lepton candidates, denoted by  $S_T$ , helps in reducing the backgrounds while retaining most of the signal. The other variable used to increase the signal significance is the invariant mass of

---

<sup>2</sup>  $E_T^{iso}/p_T^\mu \leq 0.3$ , where  $p_T$  is muon candidate's transverse momentum and  $E_T^{iso}$  is energy detected in the calorimeters in a cone of  $\Delta R = \sqrt{(\Delta\eta^2 + \Delta\phi^2)} = 0.2$  around muon candidate's reconstructed trajectory.

the two leptons,  $M_{ll}$ . The distributions of these two variables for the first generation channel are shown in Fig. 2.

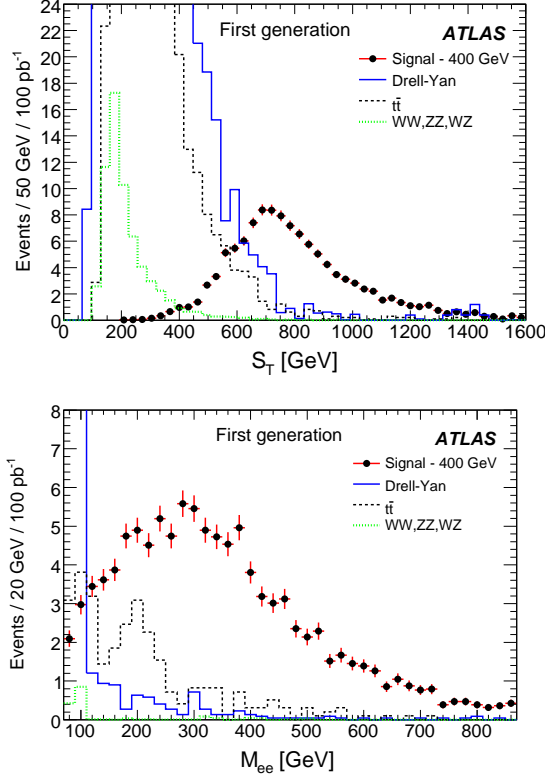


Figure 2:  $S_T$  (top) and  $M_{ee}$  of the selected electron pair after  $S_T$  requirement (bottom) in 1st gen. leptoquark MC events ( $m_{LQ} = 400$  GeV). Both distributions are normalized to  $100 \text{ pb}^{-1}$  of integrated  $pp$  luminosity.

After applying optimized selection on these two variables,  $S_T$  and  $M_{ll}$ , relative contributions from the background processes from  $t\bar{t}$ ,  $Z/DY$ , diboson and multijet are 22%, 7%, 0.4% and 18%, respectively. Partial cross-section for the signal and the background processes passing the selection criteria are shown in tables I and II for the first and second generation channels, respectively. Figure 3 shows the invariant masses<sup>3</sup> of the reconstructed leptoquark candidates before and after background suppression criteria are applied to the MC data.

### 2.3. Sensitivity and Discovery Potential

ATLAS's sensitivity to leptoquark signal for a 400 GeV mass hypothesis and with an integrated  $pp$  luminosity of  $100 \text{ pb}^{-1}$  is summarized in Fig. 4. The

<sup>3</sup>These distributions contain two entries per event corresponding to the two reconstructed leptoquark candidates.

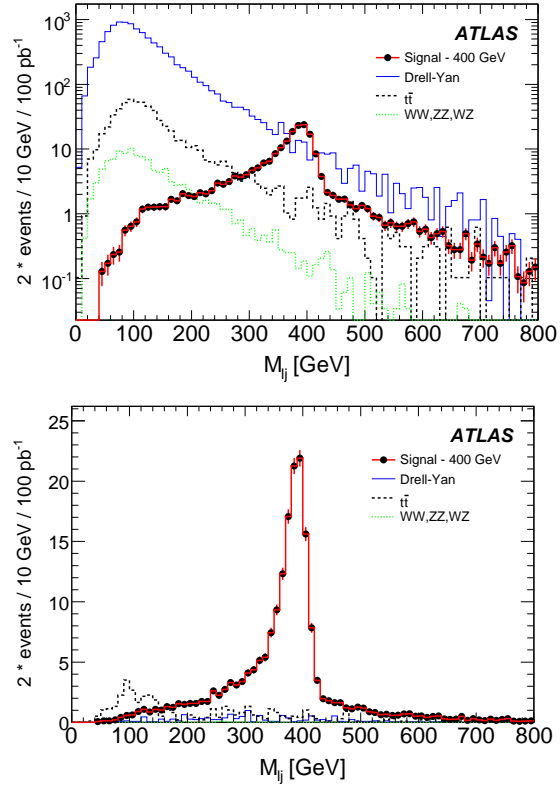


Figure 3: Reconstructed electron-jet invariant mass for 1st gen. leptoquark ( $m_{LQ}=400$  GeV) in signal and background MC events after baseline selection (top) and after additional selection criteria based on  $S_T$  and  $m_{ll}$  (bottom) have been applied. Both distributions are normalized to  $100 \text{ pb}^{-1}$  of integrated  $pp$  luminosity.

cross-sections include systematic uncertainties of 50%. Leptoquark-like events in the ATLAS detector are triggered by single leptons with an efficiency of 97%. ATLAS is sensitive to leptoquark masses of about 565 GeV and 575 GeV for 1st and 2nd generations, respectively, at the given luminosity of  $100 \text{ pb}^{-1}$  provided the predicted cross-sections for the pair production of leptoquarks are correct.

### 3. Search for $W_R$ bosons and heavy Majorana neutrinos

$W_R$  bosons are the right-handed counterpart of the SM  $W$  bosons. These right-handed intermediate vector bosons are predicted in LRSMs and can be produced at the LHC in the same processes as the SM's  $W$  and  $Z$ . They decay into heavy Majorana neutrinos. The Feynman diagram for  $W_R$  production and subsequent decay to Majorana neutrino is shown in Fig. 5.

This section describes the analysis of  $W_R$  production and its decays  $W_R \rightarrow eN_e$  and  $W_R \rightarrow \mu N_\mu$ , fol-

Table III LRSM dielectron analysis. Partial cross-section (pb) that remains after each selection criterion for the dielectron channel.

Physics sample	Before selection	Baseline selection	$M(ejj) \geq 100 \text{ GeV}$	$M(eejj) \geq 1000 \text{ GeV}$	$M(ee) \geq 300 \text{ GeV}$	$S_T \geq 700 \text{ GeV}$
LRSM_18_3	0.248	0.0882	0.0882	0.0861	0.0828	0.0786
LRSM_15_5	0.470	0.220	0.220	0.215	0.196	0.184
$Z/DY \geq 60 \text{ GeV}$	1808.	49.77	43.36	0.801	0.0132	0.0064
$t\bar{t}$	450.	3.23	3.13	0.215	0.0422	0.0165
VB pairs	60.94	0.583	0.522	0.0160	0.0016	0.0002
Multijet	$10^8$	20.51	19.67	0.0490	0.0444	0.0444

Table IV LRSM dimuon analysis. Partial cross-section (pb) that remains after each selection criterion for the dimuon channel.

Physics sample	Before selection	Baseline selection	$M(\mu jj) \geq 100 \text{ GeV}$	$M(\mu\mu jj) \geq 1000 \text{ GeV}$	$M(\mu\mu) \geq 300 \text{ GeV}$	$S_T \geq 700 \text{ GeV}$
LRSM_18_3	0.248	0.145	0.145	0.141	0.136	0.128
LRSM_15_5	0.470	0.328	0.328	0.319	0.295	0.274
$Z/DY \geq 60 \text{ GeV}$	1808.	79.99	69.13	1.46	0.0231	0.0127
$t\bar{t}$	450.	4.17	4.11	0.275	0.0527	0.0161
VB pairs	60.94	0.824	0.775	0.0242	0.0044	0.0014
Multijet	$10^8$	0.0	0.0	0.0	0.0	0.0

lowed by the decays  $N_e \rightarrow eq'\bar{q}$  and  $N_\mu \rightarrow \mu q'\bar{q}$ , which are detected in final states with (at least) two leptons and two jets. The two leptons can be of either same-sign or opposite-sign charge due to the Majorana nature of neutrinos. This analysis in both the dielectron and the dimuon channels has been performed without separating dileptons into same-sign and opposite-sign samples.

Studies [6] of the discovery potential for  $W_R$  and Majorana neutrinos  $N_e$  and  $N_\mu$  have been performed using MC samples where  $M(N_l) = 300 \text{ GeV}$ ;  $M(W_R) = 1800 \text{ GeV}$  (referred to as LRSM\_18\_3) and  $M(N_l) = 500 \text{ GeV}$ ;  $M(W_R) = 1500 \text{ GeV}$  (referred to as LRSM\_15\_5), simulated with PYTHIA according to a particular implementation [9] of LRSM [10]. The production cross-sections  $\sigma(pp(14 \text{ TeV}) \rightarrow W_R X)$  times the branching fractions ( $W_R \rightarrow lN_l \rightarrow lljj$ ) are 24.8 pb and 47 pb for LRSM\_18\_3 and LRSM\_15\_5, respectively.

### 3.1. Reconstruction and objects selection

Signal event candidates are reconstructed using two electron or muon candidates and two jets that pass the standard selection criteria as discussed in section 2.1. The two signal jet candidates are combined with each of the signal leptons and the combination that gives the smaller invariant mass is assumed to be the new

heavy neutrino candidate. The other remaining lepton is assumed to come directly from the decay of the  $W_R$  boson. If signal electrons and signal jets overlap in  $\Delta R$  within 0.4 then, to avoid double counting, only the two signal jets are used to reconstruct the invariant masses of the heavy neutrino candidate and  $W_R$ .

### 3.2. Background Studies

The main backgrounds to the LRSM analyses studied here are the same as mentioned in section 2.2. The same background suppression criteria as in the lepto-quark analyses are also effective here, namely  $S_T$  and  $m_{ll}$ . The distributions of these two variables for the dimuon channel are shown in Fig. 6. Partial cross-section for the signal and the background processes passing the selection criteria are shown in tables III and IV for the dielectron and dimuon channels, respectively. Figure 7 shows the invariant mass of the reconstructed  $W_R$  candidates before and after background suppression criteria are applied to the MC data.

### 3.3. Sensitivity and Discovery Potential

Signal significance for  $W_R$  analyses in the dielectron and dimuon channels as a function of integrated  $pp$  luminosity at 14 TeV is summarized in Fig. 8. The results include systematic uncertainty of 45% and 40% for dielectron and dimuon channel, respectively. The

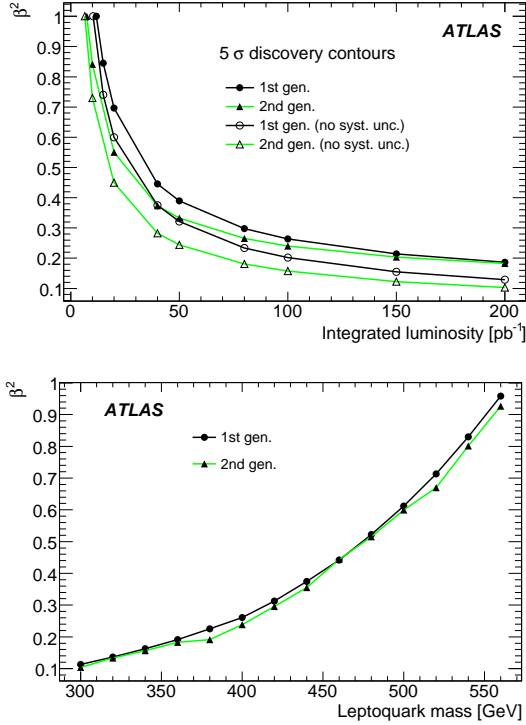


Figure 4:  $5\sigma$  discovery potential for 1st and 2nd gen. 400 GeV scalar leptoquark versus  $\beta^2$ , with and without background systematic uncertainty (top). Minimum  $\beta^2$  of scalar leptoquark versus leptoquark mass at  $100 \text{ pb}^{-1}$  of integrated  $pp$  luminosity at  $5\sigma$  (background systematic uncertainty is included) (bottom).

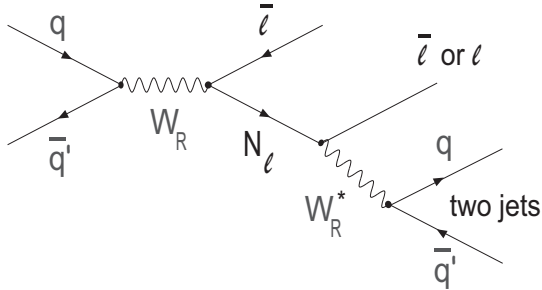


Figure 5: Feynman diagram for  $W_R$  production and its decay to the Majorana neutrino  $N_\ell$  at the LHC.

events in this analysis are also triggered by single leptons with an efficiency of 97%.

## 4. Conclusions

Dilepton-jet based final states have been discussed in both electron and muon channels. Discovery potential for leptoquarks and LRSM with early LHC data have been investigated with the predicted cross-sections for these models. Assuming a  $\beta = 1$ , both 1st

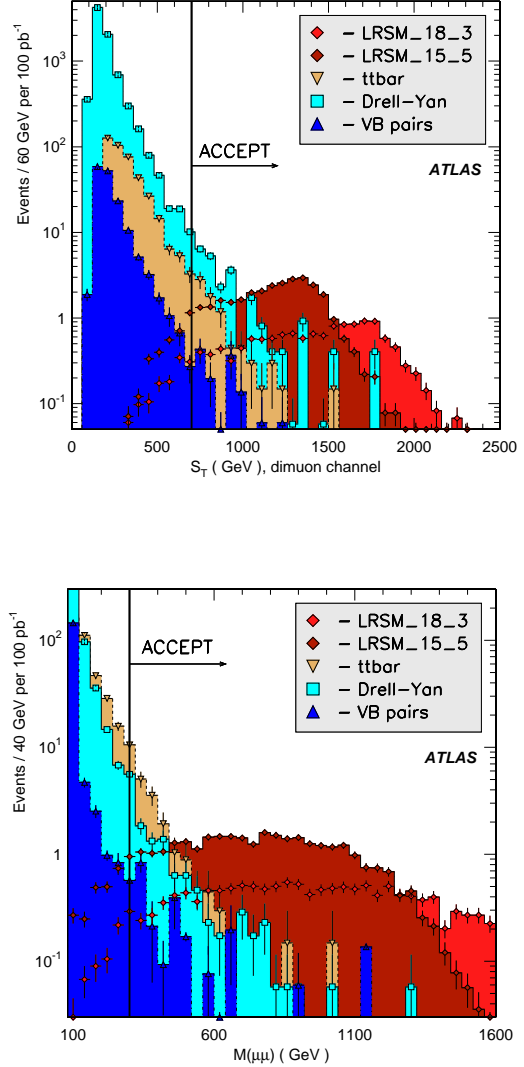


Figure 6: LRSM analysis. The distributions of  $S_T$  (top) and  $M(\ell\ell)$  (bottom) for signals and backgrounds normalized to  $100 \text{ pb}^{-1}$  of integrated  $pp$  luminosity after baseline selection in the dimuon analysis.

and 2nd generations leptoquarks could be discovered with masses up to 550 GeV with  $100 \text{ pb}^{-1}$  of data. Two LRSM mass points LRSM\_18\_3 and LRSM\_15\_5 for the  $W_R$  bosons and heavy Majorana neutrinos have been studied. The discovery of these new particles with such masses would require integrated luminosities of  $150 \text{ pb}^{-1}$  and  $40 \text{ pb}^{-1}$ , respectively.

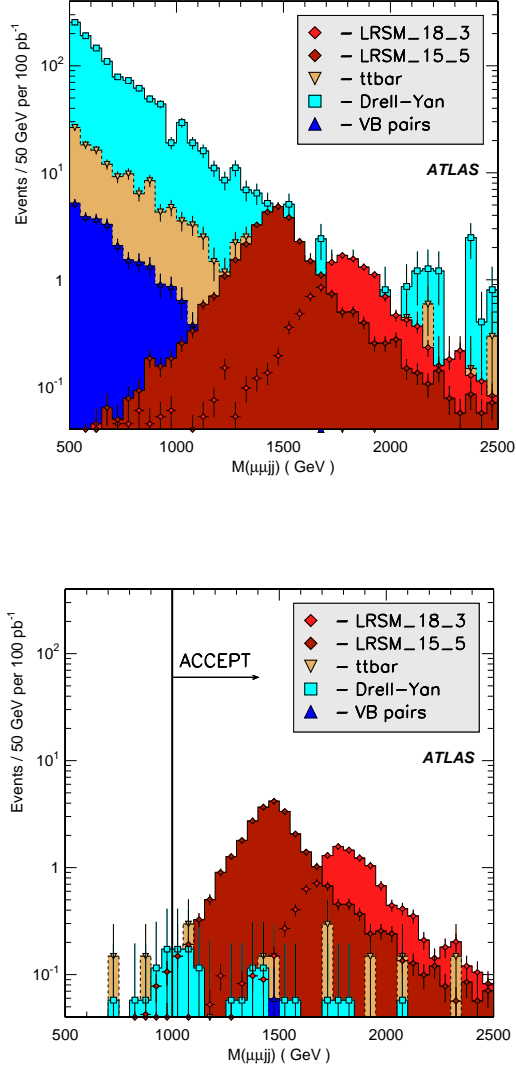


Figure 7: LRSB analysis. The distributions of the reconstructed invariant masses for  $W_R \rightarrow \mu N_\mu$  candidates in background and signal (LRSB\_18\_3 and LRSB\_15\_5) events before (top) and after (bottom) background suppression is performed in dimuon channel analysis. Both distributions are normalized to  $100 \text{ pb}^{-1}$  of integrated  $pp$  luminosity.

## References

- [1] Pati, J. C. and Mohapatra, R. N., Phys. Rev. D **11**, 566 (1975).
- [2] Mohapatra, R. N. and Senjanović, G., Phys. Rev. D **23**, 165 (1981).
- [3] Buchmüller, W. and Wyler, D., Phys. Lett. B **177**, 377 (1986).
- [4] Georgi, H. and Glashow, S. L., Phys. Rev. Lett. **32**, 438 (1974).

- [5] Leurer, M., Phys. Rev. D **49**, 333 (1994).
- [6] Aad, G. *et al.* [The ATLAS Collaboration], arXiv:0901.0512 [hep-ex].
- [7] T. Sjöstrand, *et al.*, JHEP **05** (2006) 026.
- [8] Kramer, M. *et al.*, Phys. Rev. D **71**, 057503 (2005).
- [9] Ferrari, A. *et al.*, Phys. Rev. D **62**, 013001 (2000).
- [10] Huitu, K. *et al.*, Nuc. Phys. B **487**, 27 (1997).

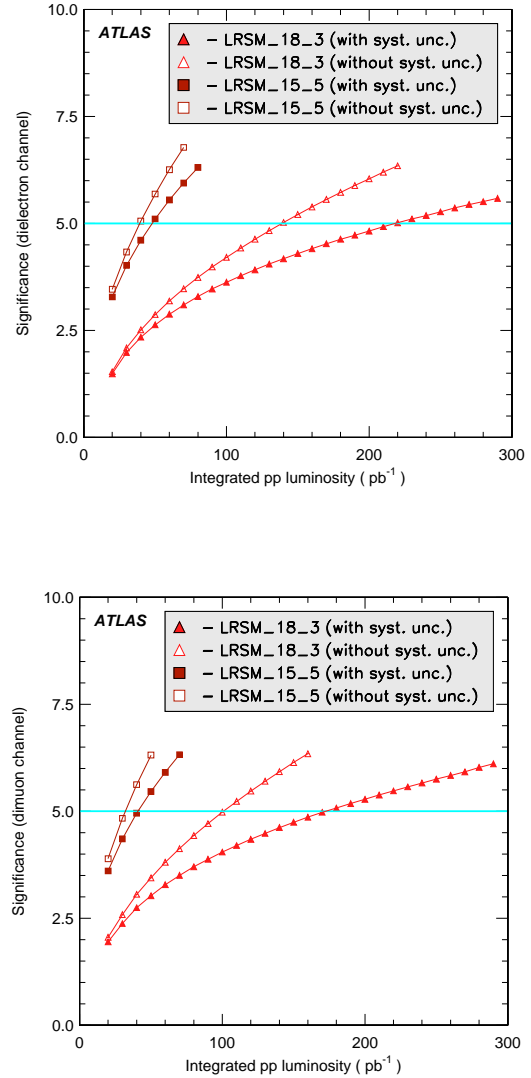


Figure 8: LRSB analysis. Expected signal significances versus integrated  $pp$  luminosity for  $N_e$ ,  $N_\mu$  and  $W_R$  mass hypotheses, according to signal MC samples LRSB\_18\_3 and LRSB\_15\_5. Open symbols show sensitivities without systematic uncertainties. Sensitivities shown with closed symbols include an overall relative uncertainty of 45% (40%), estimated for background contributions in the dielectron (dimuon) analysis.